Supporting Information for the manuscript:

On the Catalytic Mechanism of Polysaccharide Lyases: Evidence of His and Tyr Involvement in Heparin lysis by Heparinase I and the Role of Ca2+

Carolina R. Córdula[‡¹], Marcelo A. Lima[‡ƒ¹], Samuel K. Shinjo[‡], Tarsis F. Gesteira[‡†], Laércio Pol-Fachin[¤], Vivien J. Coulson-Thomas[‡¥], Hugo Verli[¤], Edwin A. Yates[ƒ‡], Timothy R. Rudd[¶ƒ], Maria A. S. Pinhal[‡]; Leny Toma[‡], Carl P. Dietrich[‡], Helena B. Nader[‡²], and Ivarne L. S. Tersariol[‡§²]

[‡]Disciplina de Biologia Molecular, Departamento de Bioquímica, Universidade Federal de São Paulo, Escola Paulista de Medicina, Rua Três de Maio, 100, CEP 04044-020, São Paulo, SP, Brazil, [ƒ] Department of Structural and Chemical Biology, University of Liverpool, Crown Street, Liverpool, L69 7ZB, UK, [¶] Diamond Light Source Ltd., Harwell Innovation Campus, Didcot, Oxfordshire, OX11 ODE, UK, ¤Centro de Biotecnologia, Universidade Federal do Rio Grande do Sul, Av Bento Gonçalves 9500, CP 15005, Porto Alegre 91500-970 RS, Brazil and [§]Centro Interdisciplinar de Investigação Bioquímica, Universidade de Mogi das Cruzes, Prédio I, Centro de Ciências Tecnológicas, sala 1S-15, Av. Dr. Candido X. de Almeida Souza 200, CEP 08780-911, Mogi das Cruzes, SP, Brazil. [1]joint first authors, [2]joint senior authors

Contents:

Methodology

Heparinase I cloning: The gene coding heparinase I was obtained from *F. heparinum* genomic DNA by PCR, using the forward primer 5'GGGCTCGAGCAGCAAAAAAAATCCGG3' and the reverse primer 5'GGATCCCTATCTGGCAGTTTCGCTG3'21. The amplified PCR product was inserted into pET 14b plasmid (Novagen) treated with XhoI/ BamHI restriction enzymes that resulted in heparinise I with an N-terminal His6 tag followed by a thrombin cleavage site. The fragment insertion was verified by DNA sequencing (Amershan).

Recombinant heparinase I (r-heparinase I) expression and purification: rHeparinase I was expressed in Escherichia coli Rosetta-gami (DE3) pLysS cells. The expression was induced by 0.5 mM IPTG at an O.D.600 of 0.5 and 18°C. The cells were grown overnight and, after that, harvested by centrifugation at 4,500 rpm for 15 min, at 4°C. The cells pellet were suspended in lyses buffer (50 mM HEPES, pH 8.0, 150 mM NaCl, 1% Triton X-100, 1 mM benzamidine and 40 mM imidazole) and sonicated (4°C, 80mHZ, 5 cycles of 30 sec with 30 sec intervals). The lysate was centrifuged at 36,000 x g for 1 hour at 40C. The cleared supernatant was incubated with 1 mL Ni-NTA beads (Invitrogen) pre-equilibrated with lyses buffer. r-Heparinase I was eluted with 300 mM imidazole in 50 mM HEPES pH 8.0, and 150 mM NaCl and detected by SDS-PAGE, immunoblotting using Anti-His antibody (GE-Healthcare) and enzymatic activity. Centricon YM-100 (Millipore Corp.) was used for concentrate the eluted fractions and change the buffer to 50 mM Tris-HCl pH 8.0. His tag was cleaved by 5 hours incubation with bovine thrombin immobilized on agarose resin (Sigma) at 18°C, and removed by incubation with 200 µL Ni-NTA resin. r-Heparinase I present in the non-retained fractions was collected and its buffer was changed to 50 mM HEPES pH 8.0 and 150 mM NaCl by ultracentrifugation. Then, recovered proteins were loaded on a Macro-Prep High Q Support anion exchange column (Bio-Rad) and eluted with 500 mM NaCl. rHeparinase I was detected in non-retained fraction by SDS-PAGE and enzymatic activity (Figure S4).

Octasaccharide Topology Construction and Energy Contour Plot Calculation: The conformational description of the glycosidic linkages associated to the octasaccharides in this study was obtained by building the composing fragments using MOLDEN software (Schaftenaar and Noordik, 2000). These structures were then submitted to the PRODRG server (Schuttelkopf and van Aalten, 2004), and initial geometries and crude topologies retrieved. Thereafter, the octasaccharide topologies were further modified to include some refinements, such as: (1) improper dihedrals, employed to preserve the

conformational state of the hexopyranose rings in 4C1 (D-GlcN, D-GlcA), 1C4 (L-IdoA) forms; (2) proper dihedrals, as described in GROMOS96 43a1 force field for glucose, in order to support stable simulations (Pol-Fachin et al., 2009), and (3) Löwdin HF/6-31G** derived atomic charges, which were either obtained from previous works (Löwdin, 1950; Becker et al., 2005; Pol-Fachin et al., 2009). The conformational description of glycosidic linkages was acquired by varying ϕ and Ψ angles, between two consecutive monosaccharide residues, from -180 to 150 degrees in 30 degree steps, generating a total of 144 conformers for each linkage, as previously described (Pol-Fachin et al., 2009). A constant force was employed restricting only ϕ and Ψ proper dihedrals during the energy minimization in each of the aforementioned values, enabling the search of conformational space associated to the linkage. Thereafter, using the minimized output conformations, a series of MD simulations were performed for 20 picoseconds (ps) at 10 K, with an integration step of 0.5 femtoseconds (fs), broaden the search for minimum-energy states. The relative stabilities of each conformation, obtained from the 10 K MD last frame, were therefore used to construct the relaxed energy contour plots thereby, representing the conformation of each glycosidic linkage.

Docking Procedures: AutoDock4.2 was used as grid-based docking procedure (Morris et al., 1998). A 3D-model of the heparinase molecule was built using MODELLER 9v1 (Fiser and Sali, 2003), using the crystal structure of heparinase II (PDB ID 2FUQ) as template (Shaya et al., 2010). The best structure for each model was selected based on the Discrete Optimized Protein Energy (DOPE) model score (Shen and Sali, 2006). Energy minimization and molecular dynamics calculations of the models were performed using GROMACS simulation suite, version 4.5.1 (Van Der Spoel et al., 2005) and GROMOS96 43a1 force field (Peng et al., 1996). The Löwdin atomic charges for the ssacharide were employed, as previously calculated for sulfated saccharides, and all torsion angles were considered flexible (Becker et al., 2005; Becker et al., 2007; Pol-Fachin et al., 2009). The grid maps, calculated using AutoGrid, were chosen to be large enough to include active site, as well as a significant portion of the surrounding surface. The dimensions of the grids were thus 60 Å × 60 Å × 40 Å, with 0.3 Å spacing between the grid points. Docking of the disaccharide to heparinase was carried out using the empirical free energy function and the Lamarckian genetic algorithm, applying a standard protocol with an initial population of 500 randomly placed individuals, a maximum number of 2.5 x 108 energy evaluations, a 0.02 mutation rate, a 0.80 crossover rate, and an elitism value of 1, where the average of the worst energy was calculated over a window of the previous 10 generations. One hundred independent docking runs were carried out for the octasaccharide. Results were clustered according to the 0.5 Å root-mean-square deviation (RMSD) criteria (Gesteira et al., 2011).

MD Simulations: The molecular systems undergoing MD were comprised of heparinase I bound or unbound to the octasaccharide, with the addition of either Na+ or Ca+ as counter ions. Thus systems, as well as the minimum-energy conformations obtained from the energy maps for the heparin octasaccharide, were solvated in rectangular boxes using periodic boundary conditions and SPC water model (Berendsen, 1987). Counter ions (Na+, Ca+) were added to neutralize the system. The employed MD protocol was based on previous studies (Schmidt et al., 1993; Verli and Guimaraes, 2004; Becker et al., 2005). The Lincs method (Hess et al., 1997) was applied to constrain covalent bond lengths, allowing an integration step of 2 fs after an initial energy minimization using Steepest Descents algorithm. Electrostatic interactions were calculated using Particle Mesh Ewald method (Darden et al., 1993). Temperature and pressure were kept constant by coupling protein, octasaccharide, ions and solvent to external temperature and pressure baths with coupling constants of τ = 0.1 and 0.5 ps (Berendsen et al., 1984), respectively. The dielectric constant was treated as ε = 1. The systems were heated slowly from 50 to 310 in 50 K steps every 5 ps, after which, all simulations were performed a further 20ns under a constant temperature of 310K. Hydrogen bonds were defined as a maximum distance of 0.35 nm between donor-acceptor heavy atom and the acceptor atom–donor hydrogen with an angle of 30 degrees.

Equations

Equation 1: The data from Ca^{2+} activation were analyzed by non-linear regression based on the Equation 1,

$$v = \frac{V_{\max}.[SA]}{K_{SA}\left(1+\frac{[S]}{K_S}\right)+[SA]}$$

where SA is the true substrate heparin-calcium complex, S is heparin free of calcium (competitive inhibitor of heparinase I), KS_A is the true substrate heparin-calcium dissociation constant, KS is the pseudo-substrate dissociation constant (inhibitor dissociation constant), and Vmax= kcat.[E].

Equation 2: This equation was using to analyze the data from pH-dependence of kcat/KS_A and kcat:

$$\frac{\lim 10^{(pH-pK_1)}}{10^{(2pH-pK_1-pK_2)}+10^{(pH-pK_1)}+1}$$

Equation 3: The data from influence of pH upon 1/KS_A were analyzed based in Equation 3,

$$\frac{\lim_1+\lim_2.10^{(pH-pKa)}}{10^{(pH-pK_a)}+1}$$

Equation 4: The temperature effect on the pKa of any dissociable group is the consequence of the enthalpy of ionization. The effect of changing temperature on pKa is given by integrated Van't Hoff relationship:

$$\mathrm{p}Ka = \frac{\Delta H_{ion}}{2.3R}\frac{1}{T} - \frac{\Delta S_{ion}}{2.3R}$$

Equation 5: The effect of temperature on the rate of product formation (kcat) or on the rate of enzyme inactivation (kdenat) was described by the integrated form of the Arrhenius relationship,

$$\log\frac{k_2}{k_1} = \frac{Ea}{2.3R}\left(\frac{T_2 - T_1}{T_2 T_1}\right)$$

where k2 and k1 are the specific reaction rate constants at T2 and T1, respectively.

Equation 6: This equation relates the dependence of maximum speed (Vmáx) of heparinase I to the fraction of deuterium, n, in a mixture of solvents (H_2O/D_2O).

$Vn = VH\ (1 - n + n\emptyset 1)$

where Vn and VH are the Vmáx in a binary solvente system D_2O/H_2O respectively, and Ø1 is the factor of proportionality between the solvents.

Equation 7: These equations define the Φ

$\Phi = O5–C1–OX–CX$

Equation 8: These equations define the Ψ

$\Psi = C1–OX–CX–C(X - 1)$

where Vn and VH are the Vmáx in a binary solvente system D_2O/H_2O respectively, and Ø1 is the factor of proportionality between the solvents.

Abbreviations

ΔU-GlcNS,6S, D-glucuronic acid-(1→4)-2-deoxi-2-sulfamine-D-glucopyranose 6-O-sulfate; ΔU,2S-GlcNS,6S, 2-sulfo-L-iduronic acid-(1→4)-2-deoxi-2- sulfamine-D-glucopyranose 6-O-sulfate, ΔU,2S-GlcNS,6S-GlcUA-GlcNS,6S, 2-sulfo-L-iduronic acid-(1→4)-2-deoxi-2- sulfamine-D-glucopyranose 6-O-sulfate-(1→4)-D- glucuronic acid-(1→4) -2-deoxi-2-sulfamine-D-glucopyranose 6-O-sulfate.

Results

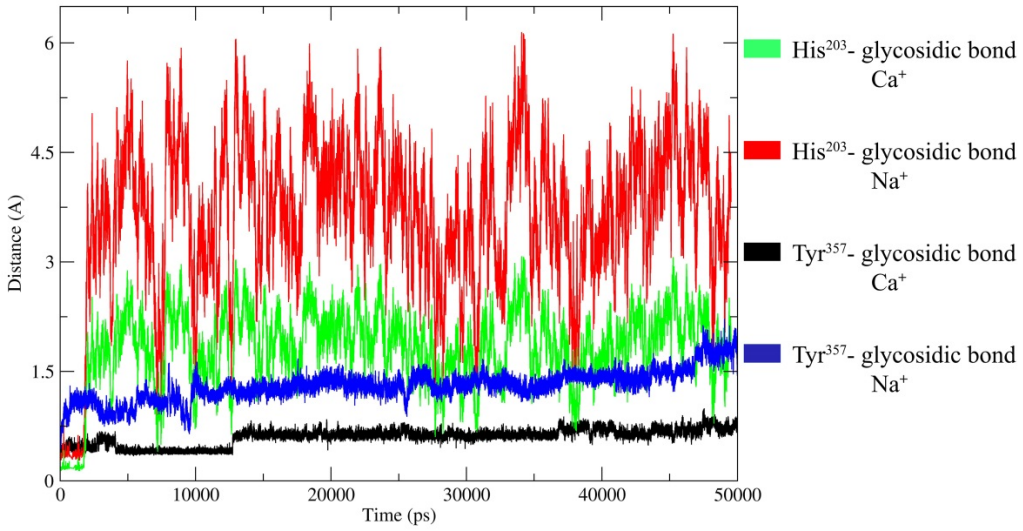

Figure S1: Molecular Dynamic (MD) simulation of the heparinase I-heparin (ES) complex. The distance to the glycosidic linkage by the catalytic His203 (green and red) and Tyr357 (black and blue) residues during MD simulations of the heparinase I-heparin (ES) complex in the presence of Na+ (blue and red) or Ca2+ (black and green). The four systems displayed the following distance trends over 50 ns: the presence of Na+ led to higher distance for Tyr357 to the substrate (1.8 ± 0.6 Å on average) than Ca2+ (0.8 ± 0.1 Å on average), and for His203, gave higher distance values for Na+ (3.9 ± 1.4 Å on average) than for Ca2+ (1.5 ± 0.2 Å on average).

Molecular dynamics data clearly suggest that Ca^{2+} restricts the flexibility of the complex ES and stabilizes one of at least two possible conformations of heparin within the active site of heparinase I leading to formation of the ternary productive heparinase I-Ca^{2+}-heparin complex. Molecular dynamics simulations suggested that, when Na^{+} was bound in the ES complex, the catalytic Tyr^{357} and His^{203} residues significantly deviate from the configuration observed with Ca^{2+} bound. Although Na^{+} did not prevent the binding of heparin to the active site of the enzyme, the presence of Na^{+} perturbs the correct spatial orientation of heparin in the active site of heparinase I and thereby inhibits its catalysis. Collectively, these findings demonstrate that Ca^{2+} controls the conformational flexibility of the heparin structure during heparinase I catalysis.

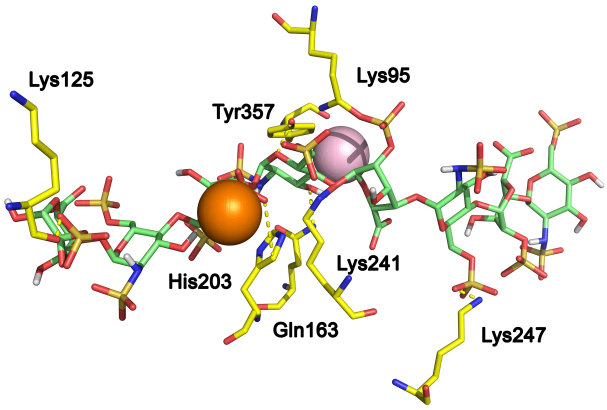

Figure S2: Representation of the complex of heparin with heparinase I. heparinase I with heparin octasaccharide substrate after 5ons dynamics simulation. The carbon atoms of heparin are in*green*, oxygen in red and sulfur in dark yellow. View of the minimum energy conformation, showing the substrate completely engulfed inside the heparinase I active site cavity: His^{203} and Tyr^{357} (dark blue for nitrogen atoms, light yellow for carbon atoms, red for oxygen atoms). Calcium atoms are represented by orange and pink spheres.

Docking experiments show that calcium ions were able to interact directly with both heparinase I and heparin simultaneously; Ca^{2+} showed pentagonalbipyramidal coordination (Fig. S2). The equatorial ligands of the pentagonalbipyramid are Oε1 (2.8 Å) and Oε2 (2.6 Å) of Glu^{228}, Oδ2 (2.3 Å) of Asp^{352}, and the backbone carbonyl oxygens of Trp^{254} (2.4 Å) and Asn^{351} (2.5 Å). The axis ligands of the bipyramid are Oγ1of Ser^{155} (2.8 Å) and a water molecule (2.6 Å). Interestingly, this calcium ion binding site did not interact with the heparin substrate. However, these results also revealed a second calcium binding site on heparinase I that recognizes the $^1C_4$ chair form of the IdoA,2S residue. Indeed, the population of the $^1C_4$ chair form of the 2-O-sulfated iduronic acid residue in heparin increased in the presence of Ca^{2+} ions compared to the presence of Na^+ ions. In this conformation, one calcium ion was able to coordinate six oxygen atoms from heparin disaccharide, four oxygens from the substrate heparin: ring oxygen from the IdoA,2S(6) residue (2.7 Å), one from glycosidic oxygen bond at C1 atom from the IdoA,2S(6) residue (2.5 Å), one from the carboxylate group from the IdoA,2S(6) residue (2.5 Å), one oxygen from the $-NSO_3$ group of the GlcNS,6S residue, one oxygen atom is from the enzyme, the Oε1 group from Gln^{229} (2.4 Å), and a water molecule (2.6 Å). Further ligation is with nitrogen (2.6 Å) from the sulfamine group from the GlcNS,6S. These data are consistent with results in the literature. Docking analysis showed that the crude interaction energy (E_{int}) of the heparin-heparinase I complex calculated in the absence of calcium ions was E_{int}= -214 ± 28 kcal/Mol. The E_{int} value of this complex did not change in the presence of calcium ions, E_{int}= -218 ± 29 kcal/Mol. These results also show that the presence of calcium ions does not affect the dissociation constant of the heparin-heparinase I complex.

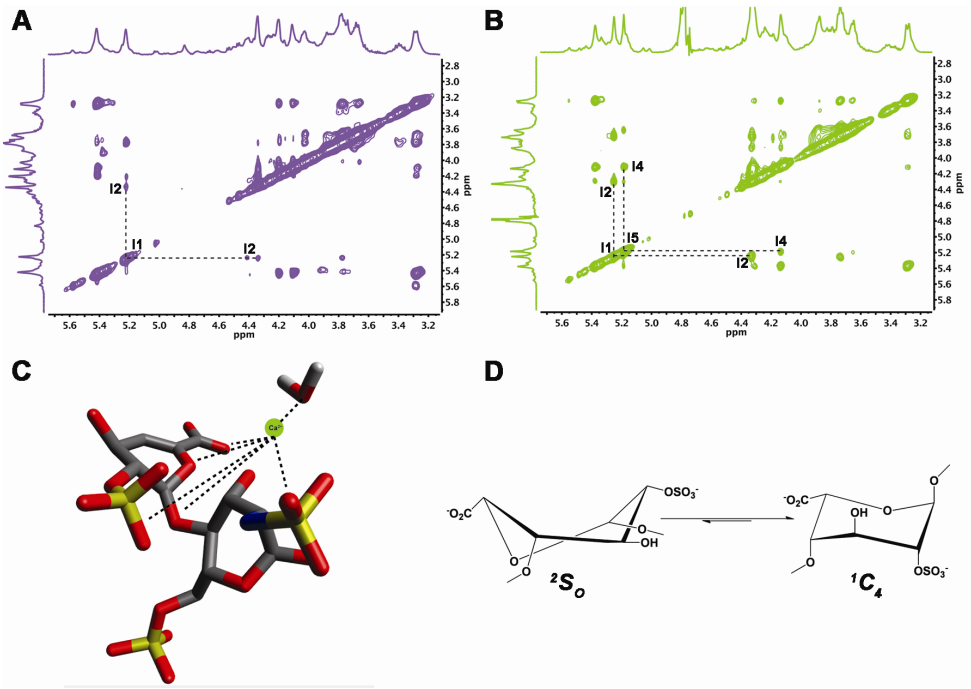

Figure S3: **A.** NOESY NMR spectrum of UFH-Na^+ highlighting the I1-I2 signal which indicates ^2S_o confomartion for the IdoA2S. **B.** NOESY spectrum of UFH-Ca^{+2} showing the increase in I4-I5 signal which corresponds to a shift in IdoA2S conformation towards $^1c_4$. **C.** Ca^{+2} coordination with the heparin trisulfated disaccharide. **D.** IdoA2S conformational equilibrium (UFH-Na^+ 60:40 (^2S_o:$^1c_4$), UFH-Ca^{+2} 20:80 (^2S_o:$^1c_4$)(Rabenstein et al, 1995).

Molecular recognition plays a central role in enzymatic catalysis although the lyases are characterized by an absence of exquisite specificity, several structures being known substrates, with varied susceptibilities . Heparinase I is known to degrade heparin in a fairly restricted way, in which the-4)-α-L-IdoA2S-α-(1→4)-D-GlcNS– sequence is recognized and depolymerized by a β-eliminative reaction. Owing to the fact that the latter heparin sequence is flexible, especially the IdoA2S residue, and that the glucosamine 6-O-sulfation is not required for catalysis, the catalytic action is dependent on the heparin topology. Such an assumption can be made based on the fact that the IdoA2S residues can adopt several conformations in solution, particularly upon protein binding and that glucosamine 6-O-sulfation is known to have only a moderate effect on the overall heparin conformation (Rudd et al, 2010). The specificity of heparinase II is quite broad where either -4)-β-D-GlucA-β-(1→4)-D-GlcNAc or -4)-β-D-GlucA-β-(1→4)-D-GlcNSO3 can serve as a substrate. Again, the NAc to NSO3 conversion does not alter the overall topology of this saccharide sufficiently to change its specificity. Calcium ions seem to be important for heparinase I action and the binding of Ca^{2+} to heparin does exhibit a degree of site-specificity involving several oxygen atoms (Fig. S3C) (Rabenstein et al, 1985 and Hricovini et al, 2010). Furthermore, evidence that cations, especially Ca^{2+} and Mg^{2+}, alter the conformation of the uronic acid of heparin and N-acetylated heparin is provided by SRCD spectra (Rudd et al, 2007), which report changes in the chiral environment of chromophores within

the carboxylate groups of the uronic acids. Additionally, as seen in Figs 3SA and 3SB (NOESY NMR spectra (Supplementary Information, S1), the binding of Ca^{2+} to heparin strongly alters the conformational equilibrium of IdoA2S residues, where a significant increase in the $^1C_4$ conformation is observed, as evinced by the increase in NOEs between I-5 and I-4 (Rabenstein et al, 1995). Other significant differences exist for interactions between several nuclei for the Ca^{2+} form, which shows that both glycosidic linkage and iduronate ring conformation change (Fig. S3D).

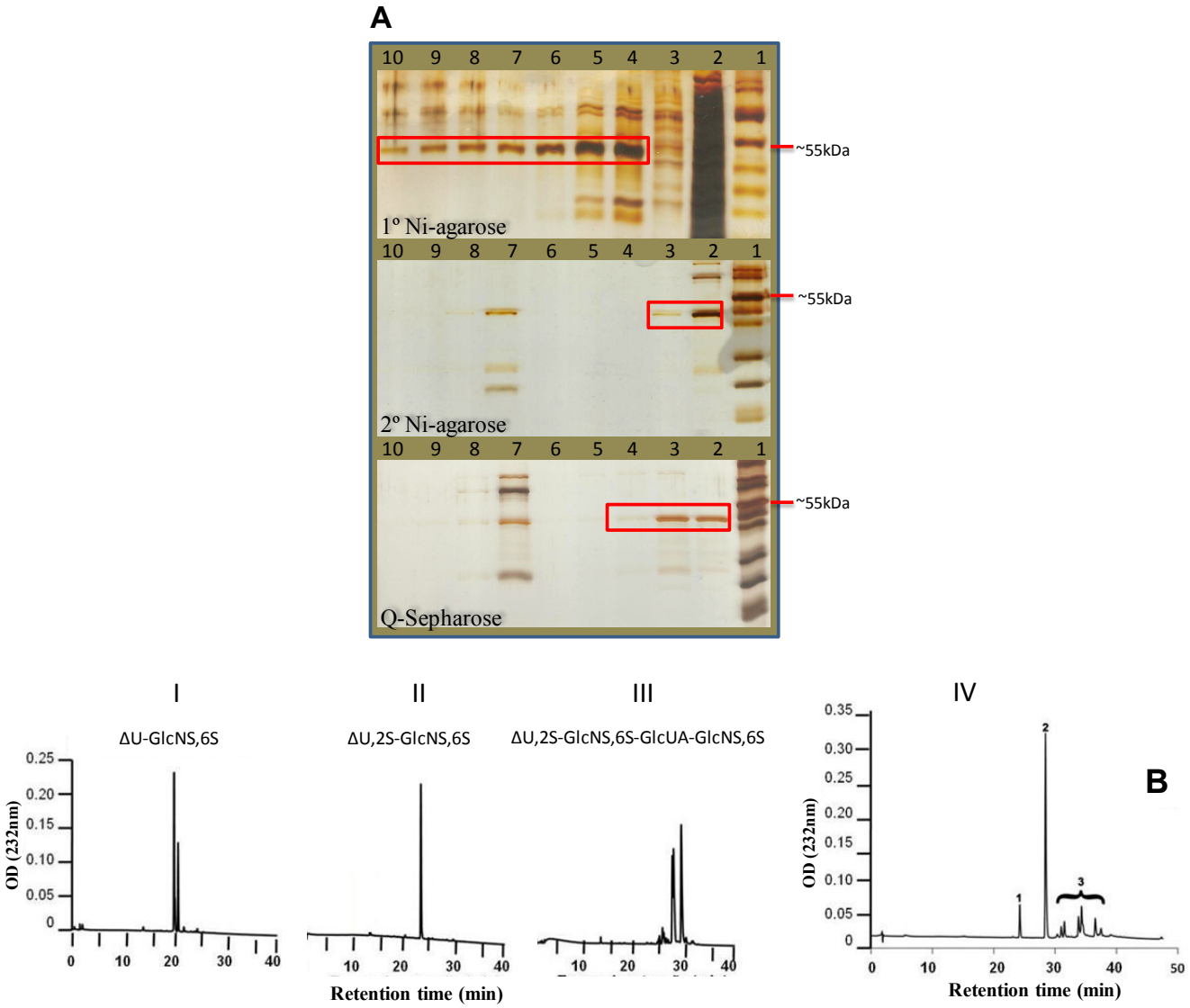

Figure S4: Expression and Purification of r-Heparinase I. **A**. SDS-PAGE of the collected chromatography fractions from r-heparinase I purification steps. **1ºNi-agarose** - affinity chromatography on nickel agarose. 1- standard molecular weight; 2 – non retained proteins; 4–10 - eluted fractions (1 mL each) in 50 mM HEPES buffer pH 8.0, 150 mM NaCl and 300 mM imidazole. **2ºNi-agarose** - affinity chromatography on nickel agarose after thrombin digestion to remove the histidine tag. 1- standard molecular weight; 2-6 – flow-through fractions (1 mL each); 7 – 10 - eluted fractions (1 mL each) in 50 mM Tris-HCl buffer pH 8.0,

150 mM NaCl and 300 mM imidazole. **Q – Sepharose** – anion exchange chromatography on Q-Sepharose resin. 1- standard molecular weight; 2-6 - non-retained proteins; 7-10 – eluted proteins on Q-sepharose resin. B. SAX-HPLC chromatography of the heparin degradation products by rheparinase. I-III- heparin degradation products by heparinase I extracted from *F. heparinum*, (I) ΔU-GlcNS,6S; (II) ΔU,2S-GlcNS,6S and (III) ΔU,2S-GlcNS,6S-GlcUA-GlcNS,6S. IV- heparin degradation products by r-heparinase I. 1 - ΔU,2S-GlcNS,6S; 2-ΔU,2S-GlcNS,6S-GlcUA-GlcNS,6S; and 3-unknow. Red square – r-heparinase I.

References

(1). Schaftenaar G, Noordik JH. J Comput Aided Mol Des. Molden: a pre- and post-processing program for molecular and electronic structures. 2000, 14(2):123-34.

(2) Schüttelkopf AW, van Aalten DM. Acta Crystallogr D Biol Crystallogr. PRODRG: a tool for high-throughput crystallography of protein-ligand complexes. 2004, 60(Pt 8):1355-63.

(3) Pol-Fachin L, Fernandes CL, Verli H. Carbohydr Res. GROMOS96 43a1 performance on the characterization of glycoprotein conformational ensembles through molecular dynamics simulations. 2009, 344(4),491-500.

(4) Löwdin, P. The Journal of Chemical Physics. On the Non-Orthogonality Problem Connected with the Use of Atomic Wave Functions in the Theory of Molecules and Crystals. 1950, 18, 11.

(5) Becker, C.F., Guimaraes, J.A., and Verli, H. Carbohydr Res. Molecular dynamics and atomic charge calculations in the study of heparin conformation in aqueous solution. 2005, 340, 1499-1507.

(6). Morris, G. M., Goodsell, D. S., Halliday, R.S., Huey, R., Hart, W. E., Belew, R. K. and Olson, A. J. J. Comput. Chem. Automated Docking Using a Lamarckian Genetic Algorithm and and Empirical Binding Free Energy Function. 1998, 19, 1639-1662.

(7) Fiser A, Sali A. Methods Enzymol. Modeller: generation and refinement of homology-based protein structure models. 2003;374:461-91.

(8) Shaya D, Zhao W, Garron ML, Xiao Z, Cui Q, Zhang Z, Sulea T, Linhardt RJ, Cygler M. J Biol Chem. Catalytic mechanism of heparinase II investigated by site-directed mutagenesis and the crystal structure with its substrate. 2010, 285(26):20051-61.

(9) Shen MY, Sali A. Protein Sci. Statistical potential for assessment and prediction of protein structures. 2006; 15(11):2507-24.

(10) Van Der Spoel D, Lindahl E, Hess B, Groenhof G, Mark AE, Berendsen HJ. J Comput Chem. GROMACS: fast, flexible, and free. 2005;26(16):1701-18.

(11) Peng, J.W., Schiffer, C.A., Xu, P., van Gunsteren, W.F., and Ernst, R.R. J Biomol NMR. Investigations of peptide hydration using NMR and molecular dynamics simulations: A study of effects of water on the conformation and dynamics of antamanide. 1996, 8, 453-476.

(12) Becker, C.F., Guimaraes, J.A., Mourao, P.A., and Verli, H. J Mol Graph Model. Conformation of sulfated galactan and sulfated fucan in aqueous solutions: implications to their anticoagulant activities. 2007, 26, 391-399.

(13) Gesteira TF, Pol-Fachin L, Coulson-Thomas VJ, Lima MA, Verli H, Nader HB. PLoS One. Insights into the N-sulfation mechanism: molecular dynamics simulations of the N-sulfotransferase domain of NDST1 and mutants. 2013; 8(8), e70880.

(14) Berendsen, H.J.C. Comput Phys Commun. Biophysical application of molecular dynamics. 1987, 44, 233-242.

(15) Schmidt, M.W., Baldridge, K.K., Boatz, J.A., Elbert, S.T., Gordon, M.S., Jensen, J.H., Koseki, S., Matsunaga, N., Nguyen, K.A., Su, S., et al. Journal of Computational Chemistry. General Atomic and Molecular Electronic Structure System. 1993, 14, 1347-1363.

(16) Verli H, Guimarães JA. Carbohydr Res. Molecular dynamics simulation of a decasaccharide fragment of heparin in aqueous solution. 2004;339(2):281-90.

(17) Hess, B., Bekker, H., Berendsen, H.J.C., and Fraaije, J.G.E.M. Journal of Computational Chemistry. LINCS: A linear constraint solver for molecular simulations. 1997, 18, 1463-1472.

(18) Darden, T., York, D., and Pedersen, L. J Chem Phys. Particle Mesh Ewald-an N.Log(N) method for Ewald sums in large systems. 1993, 98, 10089-10092.

(19) Berendsen, H.J.C., Postma, J.P.M., Vangunsteren, W.F., Dinola, A., and Haak, J.R. J Chem Phys. Molecular dynamics with coupling to an external bath. 1984, 81, 3684-3690.

(20) Rabenstein DL, R. J., Peng J. Carbohydr Res. Multinuclear magnetic resonance studies of the interaction of inorganic cations with heparin. 1995, 278, 239.

(21) Rudd TR, Y. E. Mol Biosyst. Conformational degeneracy restricts the effective information content of heparan sulfate. 2010, 6, 902.

(22) Hricovini, M. J Phys Chem B. Effect of solvent and counterions upon structure and NMR spin-spin coupling constants in heparin disaccharide. 2011, 115, 1503.

(23) Rudd TR, G. S., Skidmore MA, Duchesne L, Guerrini M, Torri G, Cosentino C, Brown A, Clarke DT, Turnbull JE, Fernig DG, Yates EA. Glycobiology. Influence of substitution pattern and cation binding on conformation and activity in heparin derivatives. 2007, 17, 983.